*International Journal for Uncertainty Quantification*, 3 (6): 541–553 (2013)

# DESIGN-POINT EXCITATION FOR CRACK PROPAGATION UNDER NARROW-BAND RANDOM LOADING

***Maliki Moustapha, André T. Beck,* & Jean-Marc Bourinet***

*Structural Engineering Department, EESC, University of São Paulo, Av. Trabalhador São-carlense, 400, 13566-590 São Carlos, SP, Brazil*

*Original Manuscript Submitted: 4/2/2012; Final Draft Received: 9/5/2012*

*When cracks propagate under random loading, different realizations of the loading process lead to different histories of crack growth. Within all possible realizations of the random load process, the so-called design-point excitation represents that particular realization that most likely leads to failure (e.g. unstable crack growth). In this paper, the design-point excitation for random crack propagation is found under narrow-band load processes. The solution involves a spectral representation of the load process, rain-flow counting of the resulting stress ranges, crack growth computation by means of the Paris Law, and solution of a reliability problem by FORM (First Order Reliability Method). The FERUM software is used in the reliability analysis. The design-point excitation is shown to exist for narrow-band load processes. Some considerations are presented with respect to the form of this excitation. So far, no convergence has been obtained for broad-band processes.*

**KEY WORDS:** *random crack propagation, spectral representation, FORM, design-point, FERUM*

## 1. INTRODUCTION

Fatigue is one of the most common causes of failure of structural components, responsible for large part of GNP expenditures in maintenance of civil infrastructure. Fatigue is nowadays widely acknowledged as a stochastic process [1–11]. Crack propagation under random loading has been addressed by many authors [7, 12–17]. Stress ranges resulting from random loading have been recognized and modeled as random variables [12–14]. In this context, structural reliability theory has been widely used for the life-cycle management of fatigue-prone structures, including the effects of periodic non-destructive inspections, maintenance and repair, etc. Following well-developed structural reliability concepts, failure criteria are expressed in terms of limit-state functions, which divide the random variable space into failure and safety domains. In evaluation of the failure probability, the most probable failure point, also known as the design point, is particularly relevant. From all possible realizations of random variables that lead to failure, the so-called design point is that particular realization that is the most likely to occur. Because of this property, the design point is also the most appropriate point for the linearization of the limit state function, in the classical First Order Reliability Method (FORM). It is also worth noting that the correctness of the FORM result is conditioned by the fact that this point is unique, which could be difficult to verify for real applications. In a classical article, Der Kiureghian [18] has shown that, in random vibrations, the design point excitation corresponds to the mirror image of the free vibration of a dynamical system. Hence, if we are interested in the exceedance of the response with respect to a given threshold at a given time, the most likely excitation is the mirror image of the free vibration of the system when it is displaced by the same threshold at time zero. This theoretical result is extremely relevant for the design of dynamical systems subject to random excitations. To the authors' knowledge, no similar results have been obtained for crack propagation under random loading. Hence, this is the main contribution of the present paper. This paper

*Correspond to André T. Beck, E-mail: atbeck@sc.usp.br, URL: http://www.set.eesc.usp.br/public/pessoas/professor.php?id=3

2152–5080/13/$35.00  

aims at finding the so-called design-point excitation for crack propagation under random loading. The design-point excitation is that realization, among all the possible realizations of the loading process, which is most likely to lead to failure due to unstable crack growth for a given design life. After a brief introduction of the theoretical background, the design-point excitation is found for a center-cracked panel under random narrow-band loading. Four different cases are investigated. The loading process is first discretized using a spectral representation, involving deterministic functions indexed in a vector of random variable coefficients. Different time histories of the load process are obtained for each realization of the vector of random variables. Rain-flow counting is used to identify the stress ranges for each loading time history. Crack growth is computed by means of the Paris law. The problem is cast as a classical time-invariant reliability problem, involving only random variables. This reliability problem is solved by FORM using the FERUM software. The article is laid out as follows. The Fourier-series representation of the load process is presented in Section 2. Modeling of crack propagation is presented in Section 3. Formulation of the reliability problem is presented in Section 4. Application to an example problem is presented in Section 5. Results are discussed in Section 6 and concluding remarks are presented in Section 7.

## 2. SPECTRAL REPRESENTATION OF A STOCHASTIC PROCESS

### 2.1 General Formulation

Formulation of a time-invariant (random variable) reliability problem under random loading requires a representation of the loading process using series of deterministic functions indexed in random variables. Different representations are available, like the Karhunen–Loève [19, 20] expansion (spectral decomposition) or generalized chaos polynomials [21–24]. The Karhunen–Loève expansion requires the eigenvectors of the autocorrelation function, which are not available in closed form solutions for general random processes [24]. Generalized chaos polynomials are mathematical representations, not readily associated to the autocorrelation function or to the power spectrum density of the random process. Hence, in this paper, a spectral representation of the load process is considered, following Ref. [25].

In the spectral representation of a random process $S(t)$, the power spectrum density (PSD) function $G(w)$ of the process is discretized in a finite number $n$ of frequency components [25]:

$$\int_{w_a}^{w_b} G(w)\,dw \approx \sum_{k=1}^{n} G(w_k)\Delta w_k \tag{1}$$

where $w_a$ and $w_b$ are the lower and upper (truncation) frequencies, $\Delta w_k = (w_b - w_a)/n$ is the frequency interval, and $w_k$ is the $k$th frequency component. The discretized process representation is then obtained as

$$S_n(t) = \mu(t) + \sum_{k=1}^{n} G(w_k)\Delta w_k \left[V_k \cos(w_k t) + W_k \sin(w_k t)\right] \tag{2}$$

where $S_n(t)$ is the $n$-dimensional approximation of process $S(t)$, $\mu(t)$ is the process mean, and $V_k$ and $W_k$ are independent Gaussian random variables with zero means and unit variances. Usually, the representation in Eq. (2) is used to obtain realizations of the process $S_n(t)$ from those of random variable vectors $V$ and $W$. However, in the present article, the discretized random process representation is directly used in the FORM analysis, in terms of its representation by means of the random variable vectors $V$ and $W$.

The spectral representation in Eqs. (1) and (2) is valid for general stationary random processes. In the present article, only a band-limited, narrow-band load process is considered. For this process, the PSD function is constant between $w_a$ and $w_b$:

$$G(w) = \begin{cases} 0, & w < w_a \\ \dfrac{1}{w_b - w_a}, & w_a \le w < w_b \\ 0, & w_b \le w \end{cases} \tag{3}$$

In this article, the frequency range is $w_a = 2\pi - 1/2$ and $w_b = 2\pi + 1/2$. Since the mean frequency is $2\pi$, one time unit corresponds to one load cycle.

## 3. RANDOM CRACK PROPAGATION MODEL

### 3.1 Crack Propagation Law

In linear elastic fracture mechanics, the rate of crack propagation ($da/dN$) is assumed proportional to the variation in the stress intensity factor, $\Delta K$. In Fig. 1, Region I represents near-threshold crack growth. Region II represents intermediate crack propagation, where crack propagation rate is proportional to $\Delta K$ (on a log-log scale) and where a small plastic zone appears ahead of the crack tip. Region II is the range of application of linear elastic fracture mechanics. Finally, Region III accounts for the accelerated crack growth just prior to failure. Non-linear fracture mechanics concepts are required to model crack growth in this region.

In this paper, the Paris Law is used to model crack growth [26]:

$$\frac{da}{dN} = c(\Delta K)^m \tag{4}$$

where $c$ and $m$ are parameters of the Paris law. Equation (4) represents a straight line on a log–log diagram; hence it corresponds to Region II of the crack propagation rate curve (Fig. 1). Due to its simplicity (only two parameters need to be identified experimentally), the Paris law is widely employed in many applications. However, this law presents two major limitations: (a) it represents crack growth only in Region II; (b) the effect of the mean stress is not taken into account; and (c) it does not take into account the history of the loading and the resulting load interaction effects, which turn out to be of prime importance in some applications like aerospace structures. Some models have been developed for assessing such effects (Strip Yield, PREFFAS, CORPUS), but they are not considered in the present work.

### 3.2 Mean Stress Effect

Considering a test specimen subject to a cyclic loading of amplitude $S_a$, experimental results show a decrease of the structure life when a mean stress $S_m$ is added. Many fatigue models, including the Paris law considered herein, do not take directly into account the mean stress effects. Complementary crack propagation tests can be carried out in order to build the so-called Haigh diagram [27]. For a given lifetime, the Haigh diagram allows one to transform cycles of mean $S_m$ and amplitude $S_a$ into equivalent zero-mean cycles of amplitude $S_a^{eq}$. Different mathematical models of that diagram exist (Goodman, Gerber, etc.) [27]. The CETIM (Centre Technique des Industries Mécaniques) recommends the use of the bilinear model illustrated in Fig. 2. In terms of fatigue life, cycle ($S_m$, $S_a$) corresponding to point B in Fig. 2 is equivalent to the cycle ($0$, $S_a^{eq}$) represented by point A on the diagram. Following the Haigh diagram model, it can be shown that

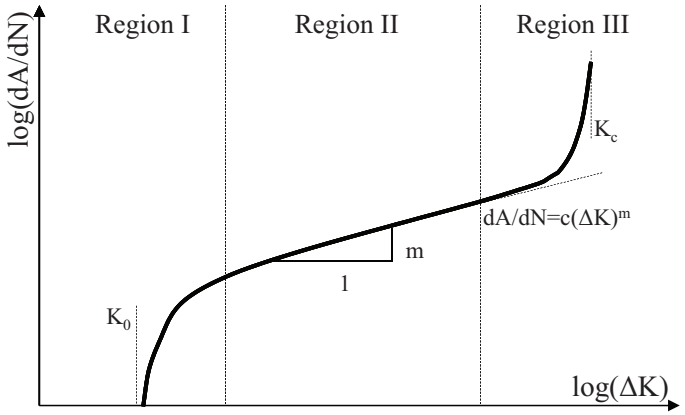


**FIG. 1:** Crack propagation rate in terms of stress ranges.

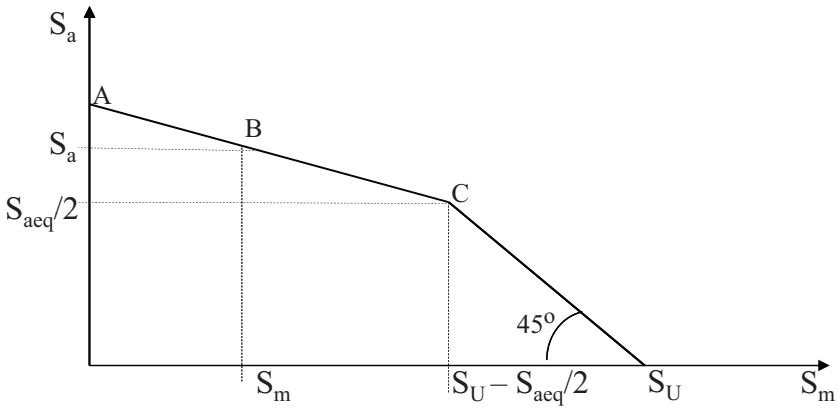


**FIG. 2:** Bilinear model of the Haigh diagram for mean stress effects.

$$S_a^{eq} = S_u + \frac{1}{2}(S_a - S_m) - \sqrt{\left(S_u + \frac{1}{2}(S_a - S_m)\right)^2 - 2S_a S_u} \tag{5}$$

where $S_u$ is the material's ultimate strength.

### 3.3 Computation of Stress Ranges from Stress Time Histories

Fatigue laws are usually obtained from constant amplitude loadings. For variable amplitude or random loadings, it is necessary to identify stress ranges from stress time histories, by means of so-called counting methods. Counting methods aim at decomposing the time history of the loading into elementary cycles. Those cycles are regrouped according to predefined stress ranges. Different counting methods exist as described in Ref. [28].

The rain-flow counting method [14] is employed in this article. This method is based on the stress–strain behavior of the material. Each extracted cycle corresponds to a closed hysteresis loop in the strain–stress curve. The rain-flow algorithm used in this article is based on the rules specified by ASTM E-1049-85 Standard [28].

### 3.4 Random Crack Propagation Models

Various random models have been developed in the literature to describe the statistical nature of crack propagation [1–8]. These models can be divided into random process and random variable models [7]. Random variable models are obtained by simply considering the parameters of deterministic crack propagation models, here $c$ and $m$ in Eq. (4), as random variables, $C$ and $M$ in this case. For random variable crack propagation models, crack growth is deterministic in time: for each realization of variables $C$ and $M$, a distinct, deterministic crack growth curve is obtained [7, 29, 30]. For random process models, the crack propagation rate is assumed to be a random process, whose value therefore changes as the crack advances in the undamaged material [2, 6, 7].

In the present article, it is convenient to adopt a random variable crack propagation model, by considering the crack propagation parameters [$C$ and $M$ in Eq. (4)], as well as the initial crack size ($A_0$), as random variables.

## 4. RELIABILITY ANALYSIS BY FORM

A structural reliability analysis consists in evaluating the failure probability of a given structure. Let $\mathbf{X}$ be a random variable vector describing the randomness in geometry, material properties, and loading. A limit-state function $g(\mathbf{X})$ is defined such that $g(\mathbf{X}) > 0$ represents the safety domain whereas $g(\mathbf{X}) \leq 0$ represents the failure domain. For random crack propagation, we consider the following limit-state function $g(\mathbf{X})$:

$$g(\mathbf{X}, t) = K_{IC} - K_I(\mathbf{V}, \mathbf{W}, A(t), C, M) \tag{6}$$

where vector $\mathbf{X}$ groups all the random variables of the problem under study $\mathbf{X} = \{\mathbf{V}, \mathbf{W}, A, C, M\}$ and where $\mathbf{V}$ and $\mathbf{W}$ are the random variable vectors representing the load process [see Eq. (2)]. The critical stress intensity factor, $K_{IC}$, is considered deterministic in the present work.

At a given time $t$, or for the corresponding number of cycles $N(t)$, the failure probability is given by

$$P_f(t) = P\left[g(\mathbf{X}, t) \leq 0\right] = \int_{g(\mathbf{x},t)\leq 0} f_{\mathbf{X}}(\mathbf{x})\, d\mathbf{x} \tag{7}$$

where $f_{\mathbf{X}}(\mathbf{x})$ denotes the joint probability density of the random vector $\mathbf{X}$. Equation (7) cannot be solved directly, because the limit-state function $g(\mathbf{x}, t) \leq 0$ is known only pointwise. An estimation of the failure probability defined at Eq. (7) can be obtained by Monte Carlo simulations, by generating samples of the random vector $\mathbf{X}$ [31, 32]. Alternatively, a common practice for assessing $P_f$ in the structural community consists in a recourse to the so-called FORM approximation method. Equation (7) is solved by conveniently introducing a mapping from the space of the original random vector $\mathbf{X}$ ($x$-space) to the so-called standard space ($u$-space) defined as follows [31, 32]:

$$\mathbf{u} = \mathbb{T}(\mathbf{x}), \qquad g_u(\mathbf{u}, t) = g(\mathbb{T}^{-1}(\mathbf{u}), t) \tag{8}$$

where all components of vector $\mathbf{u}$ are independent and identically distributed standard Gaussian random variables. This mapping can be accomplished by means of the Nataf or Rosenblatt transformations [31, 32]. In the standard space, the joint probability density $f_{\mathbf{U}}(\mathbf{u})$ is rotationally symmetric: hence, a point $\mathbf{u}^*$ on the limit state function $g_u(\mathbf{u}, t)$, which is the closest to the origin represents the most probable failure point, also known as the design point. This feature also allows the search for the design point to be cast as a constrained optimization problem:

$$\begin{aligned} \mathbf{u}^* &= \arg\min[\|\mathbf{u}\|] \\ \text{subject to } g_u(\mathbf{u},t) &= 0 \end{aligned} \tag{9}$$

From Eq. (9), $\beta = \|\mathbf{u}^*\|$ is the so-called Hasofer–Lind reliability index, which comes to be the distance between $\mathbf{u}^*$ and the origin of the standard space. The First Order Reliability Method (FORM) therefore consists in finding the design point $\mathbf{u}^*$ and approximating the original limit state function $g_u(\mathbf{u}, t)$ by a tangent hypersurface at the design point. The first-order approximation of the failure probability becomes

$$P_f(t) = P\left[g_{\mathbf{u}}(\mathbf{U}, t) \leq 0\right] \simeq \Phi(-\beta) \tag{10}$$

This approximation assumes that the most probable failure point is unique, which is true in a large number of applications. If this assumption does not hold, which may be hard to check in practice, a recourse to simulation methods represents the only acceptable alternative, despite some attempts to find multiple probable failure point of equal importance with FORM [33].

Many algorithms can be used for solving the constrained optimization problem of Eq. (9) in order to find the design point. The improved Hasofer, Lind, Rackwitz, and Fiessler (iHLRF) algorithm and Sequential Quadratic Programming (SQP) are known to be robust and efficient [34]. The iHLRF algorithm, which is used in this paper, is based on the following recursive formulas [20, 34]:

$$\mathbf{u}_{k+1} = \mathbf{u}_k + \lambda_k \mathbf{d}_k \tag{11}$$

where

$$\mathbf{d}_k = \frac{1}{\|\nabla g(\mathbf{u}_k, t)\|^2} \left(\nabla g(\mathbf{u}_k, t)\mathbf{u}_k - g_{\mathbf{u}}(\mathbf{u}_k, t)\right) \nabla g^T(\mathbf{u}_k, t) - \mathbf{u}_k$$

In Eqs. (11) and (12), $\mathbf{d}_k$ is a search direction and $\lambda_k$ is a step size, selected from minimization of an appropriate merit function [34]. In Eq. (12), $\nabla g(\mathbf{u}_k, t)$ is the gradient vector of the limit-state function with respect to $u$ evaluated at $\mathbf{u}_k$.

Example problems presented in this article are solved using the FERUM software package [35]. FERUM or "Finite Element Reliability Using Matlab" is an open-source Matlab toolbox, which was originally developed by researchers at UC Berkeley and is now maintained at the French Institute for Advanced Mechanics.

Example problems presented in this article are solved using the iHLRF algorithm. Stopping criteria must be defined in order to stop the iterative search of Eqs. (11) and (12). The following convergence criteria are employed in this article:

$$\text{g-criterion:} \quad \left| \frac{g_{\mathbf{u}}(\mathbf{u}_k, t)}{g_0} \right| < \delta_g \tag{12}$$

where $g_0$ is the initial value of the limit state-function and $\delta_g$ is a specified tolerance; and

$$\text{u-criterion:} \quad |\beta_k - \beta_{k-1}| < \delta_\beta \tag{13}$$

where $\beta_k = \|\mathbf{u}_k\|$ is the reliability index in the $k$th iteration and $\delta_\beta$ is another specified tolerance. The values $\delta_g = 10^{-2}$ and $\delta_\beta = 10^{-3}$ are adopted in this study.

It should be noted that the u-criterion is not the original criterion used in the FERUM software [35], which relates to the orthogonality between the $\mathbf{u}$ vector and the limit state function. However, due to the strong non-linearity of the limit-state function around the design point, the stopping criterion had to be modified, following Eq. (13). The orthogonality criterion, however, was checked to avoid large inaccuracies.

## 5. CENTER-CRACKED PANEL PROBLEM

A center-cracked panel under random narrow-band loading is considered as an example problem. For this problem, the stress intensity factor $K_I$ is given in closed form:

$$K_I(a,t) = S\sqrt{\pi a}Y(a) = S\sqrt{\pi a}\sqrt{\sec\left(\frac{\pi a}{b}\right)} \tag{14}$$

where $S$ is the far field stress applied at the panel boundaries and $Y(a)$ is a geometry function.

Four variants of the centre-cracked panel problem are considered in this study. In case (1) only the random process is considered: the remaining variables are assumed deterministic as presented in Table 1. In case (2) the loading process and the initial crack size are random. For case (3) the loading process and crack propagation rate are considered random. Finally, in case (4) the loading process, initial crack size, and crack propagation rate are represented as random (no correlation). The random variables for cases 2, 3, and 4 are described in Table 2.

A spectral representation of the load process is adopted, following Eq. (2). Figure 3 illustrates three crack growth time histories (case 1), obtained from three random realizations of the load process (realizations of random variables $\mathbf{V}$ and $\mathbf{W}$).

In the iterative design point search in FORM, each realization of random variable vectors $\mathbf{V}$ and $\mathbf{W}$ leads to one realization of the load process. For each load process realization, stress ranges are computed using rain-flow counting,

**TABLE 1:** Deterministic problem parameters

| Parameter | Symbol | Value | Unit |
|---|---|---|---|
| Dimension of random vectors $\mathbf{V}$ and $\mathbf{W}$ | $n$ | 100 | — |
| Mean of load process | $m_p$ | 275 | MPa |
| Paris law exponent | $m$ | 3.29 | — |
| Crack propagation rate (case 1) | $c$ | $10^{-8}$ | mm/cycle |
| Initial crack size (case 2) | $a_0$ | 8.00 | mm |
| Fracture toughness | $K_{IC}$ | 48.26 | MPa.mm$^{1/2}$ |
| Ultimate strength | $S_u$ | 455 | MPa |
| Plate width | $b$ | 152.4 | mm |

**TABLE 2:** Random resistance variables for cases 2, 3, and 4

| Random variables | Symbol | Distribution | Mean | C.O.V. | Unit |
|---|---|---|---|---|---|
| Initial crack size | $A_0$ | lognormal | 8.00 | 0.15 | mm |
| Crack propagation rate | $C$ | lognormal | $10^{-8}$ | 0.15 | mm/cycle |

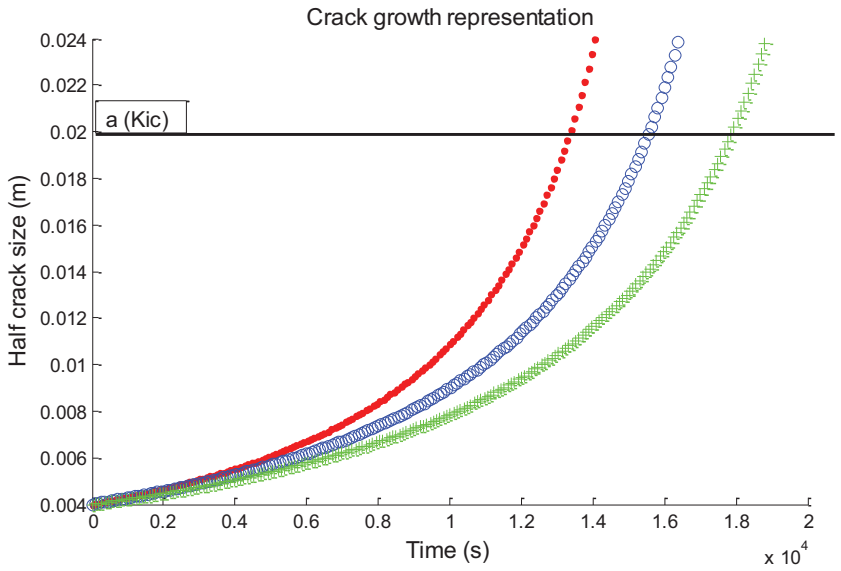


**FIG. 3:** Crack growth resulting from different realizations of vector $\mathbf{X}$.

as illustrated in Fig. 4. Crack growth is computed using the Paris Law [see Eq. (4)], with mean stress range corrections using the Haigh diagram.

## 6. RESULTS AND DISCUSSION

The iterative search for the design point was found to be highly unstable, due to strong curvatures of the limit state function. Figure 5 illustrates the matter, by showing random samples obtained via Monte Carlo simulation, for case 1 (only the load is random), and for only two random variables in the spectral representation (dimension $n = 2$ of vectors $\mathbf{V}$ and $\mathbf{W}$). The different coloring illustrates points that fall in the failure and survival domains, hence the boundary between these points is the limit state function. The point closest to the origin is the design point. Hence, strong curvature of the limit state function around the design point can be observed. Strong curvatures make convergence of the iterative FORM solution more difficult.

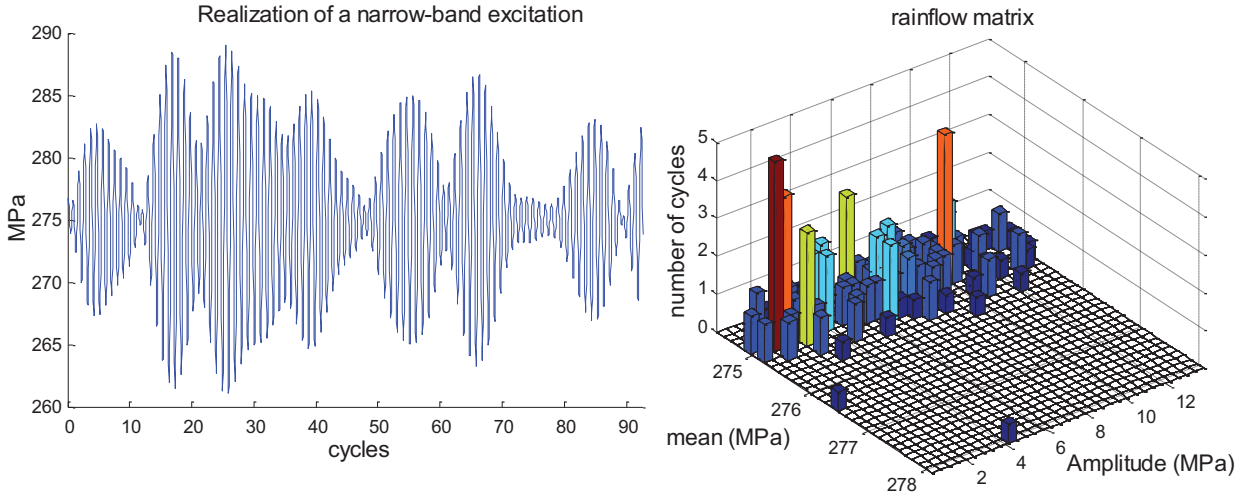


**FIG. 4:** One simulated load block time history (left) and corresponding 3D rain-flow history (right).

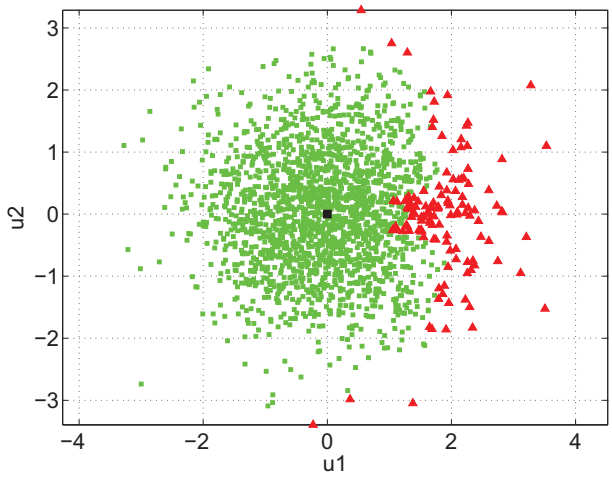


**FIG. 5:** Random samples obtained via MC simulation for case 1 and $n = 2$.

Instability and convergence difficulties were found to be stronger for larger number of random variables. Hence, the number of random variables in the spectral representation (dimension $n$ of vectors $\mathbf{V}$ and $\mathbf{W}$) had to be limited to 100. The number of time history load cycles is closely related to $n$ (actually, $n = 100$ leads to 92.63 load cycles), hence the number of load cycles had also to be limited. As a consequence, the loading process was assumed to be formed by sequences of identical load blocks, each load block consisting of around 92 load cycles. Hence, the rain-flow stress ranges (Fig. 4) correspond to one load block, and the block loading is repeated until failure.

Results for the four cases are presented in Table 3 and in Fig. 6. Results were calculated for a design life of $t_D = 9263$ cycles, which corresponds to 100 load blocks. Figure 6 illustrates the design-point excitations corresponding to one load block (left), and the corresponding design point vectors $\mathbf{V}$ and $\mathbf{W}$ (right). Design point excitations are typical of narrow-band load processes: one can observe a higher frequency signal enclosed by a lower frequency envelope. However, the main characteristic of the design point excitation, for all four cases, is that larger stress amplitudes occur early in the load block, causing the most damage "as soon as possible," whereas smaller amplitude cycles just drive the crack further, until the critical crack size is reached. This type of behavior could be expected, considering the non-linear and incremental aspect of the crack propagation law in Eq. (4).

In practical terms, the following comparison can be made. If the load process and load blocks considered herein represented an aircraft load spectrum, the most damage would occur if the pilot adopted a more aggressive flying style for the first few minutes (or hours) and a smoother style for the remaining flight time, than if he did the opposite: smoother at the beginning and more aggressive towards the finish. This comparison is of course dependent on the assumptions that are taken here for modeling the crack growth. The authors are aware that the crack propagation process is complex to model accurately in reality, due to load interactions and history effects in terms of crack tip plasticity.

Although the four design point excitations have roughly the same aspect, stress amplitudes are different. For case 2 (random $A_0$), for instance, the design point (most probable) initial crack size is 12.8 mm, significantly larger than the mean or deterministic $a_0$ (8 mm). Hence, the design point excitation stress amplitudes are smaller (in comparison to case 1). Similar behavior is observed for cases 3 and 4 (see Table 3 and Fig. 6).

Results obtained herein are highly dependent on the coefficients of variation (c.o.v.) assumed for the crack propagation random variables. Results presented herein were obtained for a c.o.v. of 15% on $A_0$ and $C$. When the c.o.v. is taken as 20%, for instance, the design-point initial crack size is very close to the critical crack size (20 mm), the design point stress amplitudes are very small and very little crack growth occurs before failure.

As mentioned before, severe convergence difficulties were encountered before the design point excitations could be identified. In part, these difficulties were avoided by an appropriate choice of starting point for the $\mathbf{V}$ and $\mathbf{W}$ random variable vectors. All the components of these vectors were fixed to the initial constant value of 0.1.

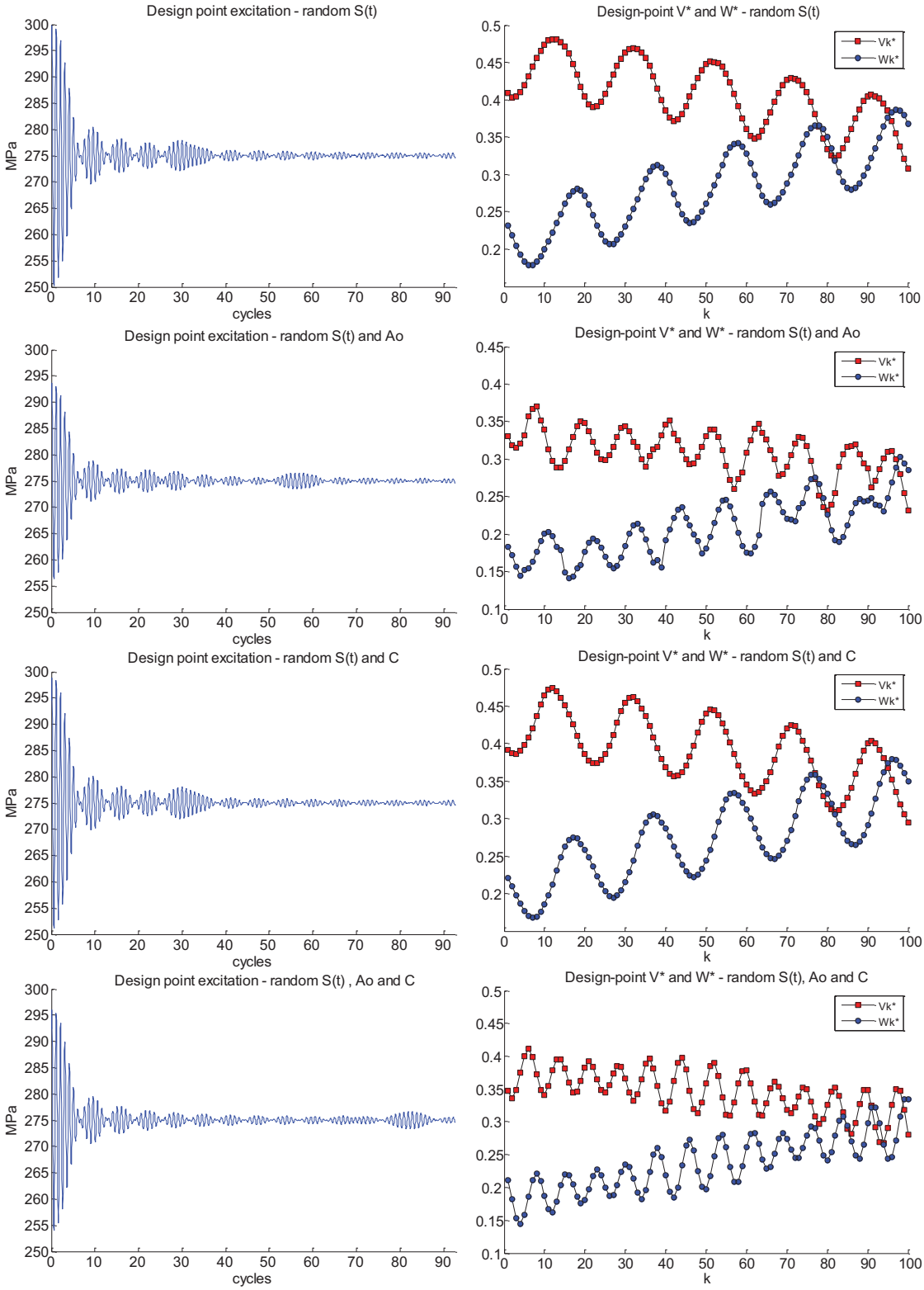


**FIG. 6:** Design point excitation (left) and corresponding design point vectors $\mathbf{V}^*$ and $\mathbf{W}^*$ (right).

**TABLE 3:** Results for the four cases

| Case | Number of it. | β | $P_f(t_D)$ | $a_0^*$ | $c^*$ | g-criterion | u-criterion |
|---|---|---|---|---|---|---|---|
| Case 1 | 5 | 4.92 | $4.38\times10^{-7}$ | — | — | $6.10\times10^{-4}$ | $8.83\times10^{-3}$ |
| Case 2 | 7 | 4.78 | $8.80\times10^{-7}$ | 12.8 | — | $9.73\times10^{-4}$ | $1.21\times10^{-2}$ |
| Case 3 | 4 | 4.83 | $6.68\times10^{-7}$ | — | $1.14\times10^{-8}$ | $4.26\times10^{-4}$ | $8.66\times10^{-3}$ |
| Case 4 | 4 | 4.62 | $1.96\times10^{-6}$ | 10.4 | $1.10\times10^{-8}$ | $2.98\times10^{-2}$ | $3.12\times10^{-3}$ |

Observation of the design point vectors $\mathbf{V}^*$ and $\mathbf{W}^*$ (right in Fig. 6) shows that smooth design points were obtained for cases 1 and 3, in contrast to cases 2 and 4 (the later presenting some noise). This, in conjunction with the convergence measures presented in Table 3, shows that convergence was smoother for cases 1 and 3. Nevertheless, considering the high non-linearity of the limit-state surface and the instabilities of the design point search, results for cases 2 and 4 were considered acceptable. A SQP algorithm, as proposed by Schittkowsky [36], was also employed, in an effort to improve the quality of convergence, but results were no better.

The observation of design point vectors $\mathbf{V}^*$ and $\mathbf{W}^*$ (right in Fig. 6, especially for cases 1 and 3) reveals that during the first part of the excitation, the cosine term ($\mathbf{V}^*$, red crosses in figure) dominates over the sine term ($\mathbf{W}^*$, blue circles in figure), since cosine coefficients are around $0.4$–$0.45$, whereas sine coefficients are around $0.2$–$0.25$. Moreover, a small phase difference can be observed between the sine and cosine terms.

Due to the convergence difficulties mentioned earlier, the design point excitation for broad-band load processes could not be identified.

Sensitivity coefficients corresponding to the four studied cases are presented in Table 4 and Fig. 7. In linear (first-order) reliability theory, these sensitivity coefficients, also known as $\alpha-$vector, represent the contribution of each random variable in the failure:

$$\alpha = -\frac{\nabla g(\mathbf{u}^*)}{\|\nabla g(\mathbf{u}^*)\|} \tag{15}$$

Since this $\alpha$-vector is unitary, a given component $(\alpha_i)^2$ represents the contribution (with respect to the unit) of the $i$th random variable in vector $\mathbf{u}$ in the failure. In Fig. 7 it is observed that the contribution of random variable parameters ($A_0$ and $C$) is quite significant. However, Table 4 presents the combined effect of vectors $\mathbf{V}$ and $\mathbf{W}$ (random process variables), which shows that the load process uncertainty also plays a significant role in the failure.

## 7. CONCLUDING REMARKS

In this article, it was proposed to identify the design-point excitation for random crack propagation under random loading. A spectral representation was adopted for the load process. Stress ranges were identified by means of rain-flow counting, and crack growth was computed using the Paris Law. Mean stress range were considered using a Haigh diagram. The limit-state function was written in terms of the stress intensity factor reaching a critical value. A center-cracked panel was considered as an example, with four cases: random load process only, random load and initial crack size, random load and crack propagation rate, and, finally, random load, initial crack size, and crack propagation rate.

Search for the design point excitation was found to be highly unstable, due to large non-linearities of the limit-state function. Hence, the design point excitation under broad-band load processes could not be found. Under band-limited,

**TABLE 4:** Sensitivity coefficients for four cases

| | $\sum_{k=1}^{100}(\alpha_{V_k})^2$ | $\sum_{k=1}^{100}(\alpha_{W_k})^2$ | $(\alpha_{A_0})^2$ | $(\alpha_C)^2$ |
|---|---|---|---|---|
| Case 1 | 0.6674 | 0.3326 | — | — |
| Case 2 | 0.5352 | 0.2587 | 0.2067 | — |
| Case 3 | 0.6403 | 0.3206 | — | 0.0391 |
| Case 4 | 0.5715 | 0.2914 | 0.1152 | 0.0228 |

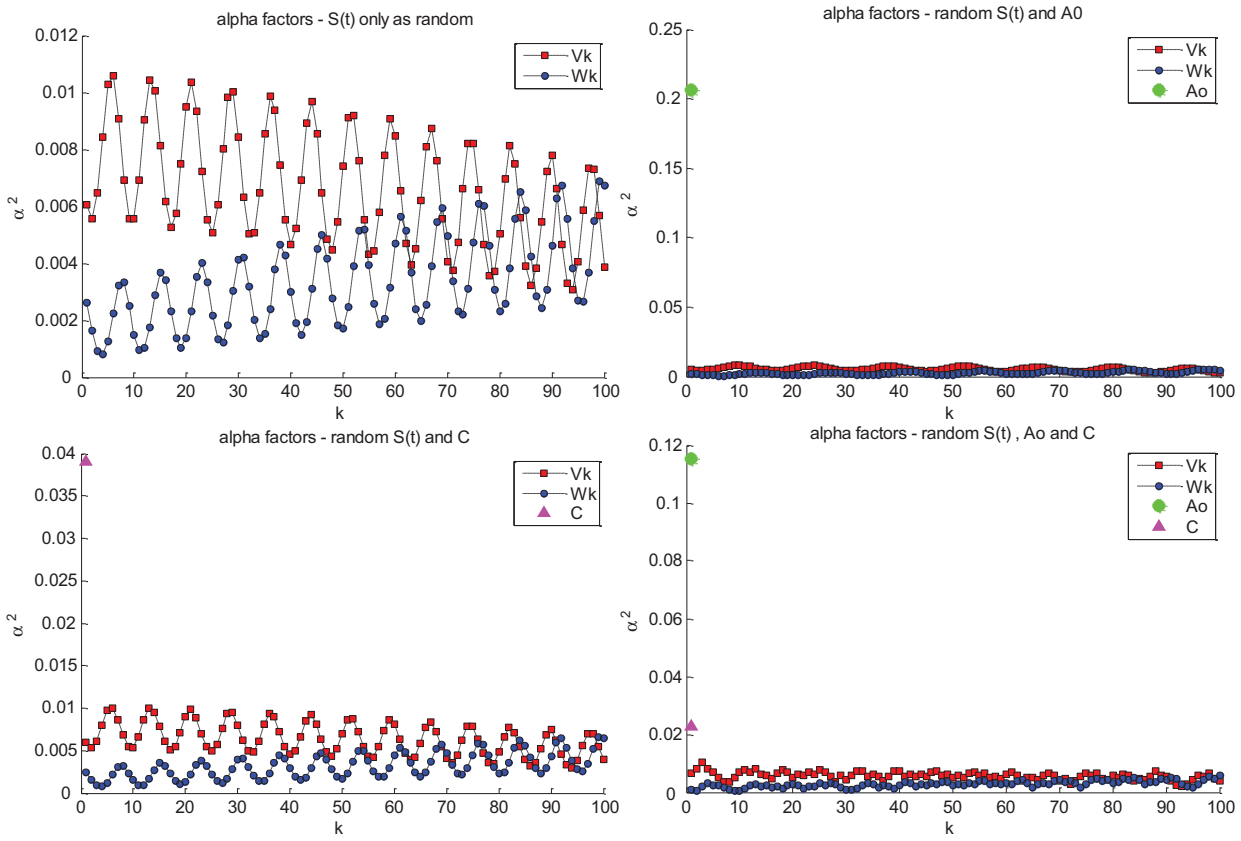


**FIG. 7:** Sensitivity coefficients for four cases investigated: random load process only (top left), random $A_0$ (top right), random $C$ (bottom left), and random $A_0$ and $C$ (bottom right).

narrow-band excitation, the design point excitation could be identified, by selecting a proper initial point for the FORM algorithm.

Under narrow-band loading, and for the four cases considered, the design point excitation was found to produce large stress cycles at the early stages of the load block, causing the most damage "as soon as possible," and smaller stress ranges towards the later part of the load block. This type of behavior could have been expected, in consideration of the non-linear and incremental aspects of the crack propagation law. However, in the present work, this type of design point excitation is shown to exist, as one possible realization of a narrow-band load process.

## ACKNOWLEDGMENT

Sponsorship of this research project by the National Council for Research and Development—CNPq (Grant No. 301679/2009-6) is greatly acknowledged.

## REFERENCES

1. Virkler, D. A., Hillberry, B. M., and Goel, P. K., The statistical nature of fatigue crack propagation, *J. Eng. Mater. Tech. (ASME)*, 101:148–153, 1979.
2. Lin, Y. K. and Yang, J. N., A stochastic theory of fatigue crack propagation, *AIAA J.*, 23:117–124, 1985.
3. Yao, J. T. P., Kozin, F., Wen, Y. K., Schuller, G. I., and Ditlevsen, O., Stochastic fatigue, fracture and damage, *Struct. Safety*, 3:231–267, 1986.

4. Ghonem, H. and Dore, S., Experimental study of the constant probability crack growth curves under constant amplitude loading, *Eng. Fract. Mech.*, 27:1–25, 1987.
5. Provan, J., *Probabilistic Fracture Mechanics and Reliability*, Martinus Nijhoff Publishers, Dordrecht, The Netherlands, 1987.
6. Sobczyk, K. and Spencer, B. F., *Random Fatigue: From Data to Theory*, Academic Press, 1992.
7. Beck, A. T. and Melchers, R. E., Overload failure of structural components under random crack propagation and loading—A random process approach, *Struct. Safety*, 26:471–488, 2004.
8. Castillo, E., Fernandez-Canteli, A., Castillo, C., and Mozos, C. M., A new probabilistic model for crack propagation under fatigue loads and its connection with Whler fields, *International Journal of Fatigue*, 32:744–753, 2010.
9. Leonel, E. D., Chateauneuf, A., Venturini, W. S., and Bressolette, P., Coupled reliability and boundary element model for probabilistic fatigue life assessment in mixed mode crack propagation, *Int. J. Fatigue*, 32:1823–1834, 2010.
10. Leonel, E. D. and Venturini, W. S., Multiple random crack propagation using a boundary element formulation, *Eng. Fract. Mech.*, 78:1077–1090, 2011.
11. Leonel, E. D., Beck, A. T., and Venturini, W. S., On the performance of response surface and direct coupling approaches in solution of random crack propagation problems, *Struct. Safety*, 33:261–274, 2011.
12. Wirsching, P. H. and Shehata, A. M., Fatigue under wideband random stresses using the rainflow method, *J. Eng. Mater. Tech. (ASME)*, 99:205–211, 1977.
13. Nagode, M. and Fajdiga, M., A general multi-modal probability distribution function suitable for the rainflow ranges of stationary random processes, *Int. J.Fatigue*, 20:211–223, 1998.
14. Bouyssy, V., Naboishikov, S. M., and Rackwitz, R., Comparison of analytical counting methods for gaussian processes, *Struct. Safety*, 12:35–57, 1993.
15. Gupta, S. and Rychlik, I., Rain-flow fatigue damage due to nonlinear combination of vector Gaussian loads, *Probab. Eng. Mech.*, 22:231–249, 2007.
16. Bengtsson, A. and Rychlik, I., Uncertainty in fatigue life prediction of structures subject to Gaussian loads, *Probab. Eng. Mech.*, 24:224–235, 2009.
17. Sarkar, S., Gupta, S., and Rychlik, I., Wiener chaos expansions for estimating rain-flow fatigue damage in randomly vibrating structures with uncertain parameters, *Probab. Eng. Mech.*, 26:387–398, 2011.
18. Der Kiureghian, A., The geometry of random vibrations and solutions by FORM and SORM, *Probab. Eng. Mech.*, 15:81–90, 2000.
19. Love, M., *Probability Theory*, 4th ed., Springer, New York, 1977.
20. Sudret, B. and Der Kiureghian, A., Stochastic finite element methods and reliability: A state-of-the-art report, Tech. Rep., Department of Civil & Environmental Engineering, University of California, Berkeley, 2000.
21. Wiener, N., The homogeneous chaos, *Am. J. Math.*, 60:897936, 1938.
22. Askey, R. and Wilson, J., Some basic hypergeometric polynomials that generalize Jacobi polynomials, *Mem. Am. Math. Soc.*, 319, 1985.
23. Xiu, D. and Karniadakis, G. E., The Wiener-Askey polynomial chaos for stochastic differential equations, *SIAM J. Sci. Comput.*, 24:619–644, 2002.
24. Ghanem, R. G. and Spanos, P. D., *Stochastic Finite Elements—A Spectral Approach*, Springer, New York, 1991.
25. Grigoriu, M., A spectral representation based model for Monte Carlo simulation, *Probab. Eng. Mech.*, 15:365–370, 2000.
26. Paris, P. C. and Erdogan, F., A critical analysis of crack propagation laws, *J. Basic Eng.*, 85:528–534, 1963.
27. Sendeckyj, G. P., Constant life diagrams—A historical review, *Int. J. Fatigue*, 23:347–353, 2001.
28. ASTM, Standard practices for cycle fatigue counting in fatigue analysis, *Designation E-1049, Metal Tests and Analytical Procedures*, pp. 836–848, 1985.
29. Nespurek, L., Bourinet, J.-M., Gravouil, A., and Lemaire, M., Some approaches to improve the computational efficiency of the reliability analysis of complex crack propagation problem, *3rd International ASRANet Colloquium*, July 2006.
30. Bourinet, J.-M. and Lemaire, M., Form sensitivities to correlation: Application to fatigue crack propagation based on virkler data, *4th International ASRANet Colloquium*, 2008.

31. Ang, A. H.-S. and Tang, W. H., *Probability Concepts in Engineering: Emphasis on Applications to Civil and Environmental Engineering*, Wiley, New York, 2007.
32. Melchers, R. E., *Structural Reliability Analysis and Prediction*, 2nd ed., Wiley, New York, 1999.
33. Der Kiureghian, A. and Dakessian, T., Multiple design points in first and second-order reliability, *Struct. Safety*, 20:37–49, 1998.
34. Liu, P. L. and Der Kiureghian, A., Optimization algorithms for structural reliability, *Struct. Safety*, 9:161–177, 1991.
35. Ferum software, July 2011, http://www.ifma.fr/FERUM.
36. Schittkowski, K., On the convergence of a sequential quadratic programming method with an augmented Lagrangian line search function, *Math. Operationsforschung Stat., Ser. Opt.*, 14:197–216, 1983.